SJÄLVSTÄNDIGA ARBETEN I MATEMATIK

MATEMATISKA INSTITUTIONEN, STOCKHOLMS UNIVERSITET

Ehrhart Polynomials of Gelfand-Tsetlin Polytopes

av

Oskar Hogman

2026 - No K7

Ehrhart Polynomials of Gelfand-Tsetlin Polytopes

Oskar Hogman

Självständigt arbete i matematik 15 högskolepoäng, grundnivå

Handledare: Per Alexandersson

2026

Abstract

Gelfand-Tsetlin patterns play an important role in combinatorics, as they are in bijection with semistandard Young tableaus, a type of Schur function. Using Gelfand-Tsetlin patterns as a number of halfspaces, one can form Gelfand-Tsetlin polytopes. In this thesis, these polytopes are examined up to a dimension of 21 and their Ehrhart polynomials are computed.

Sammanfattning

Gelfand-Tsetlinmönster spelar en viktig roll i kombinatorik, då de är i bijektion med semistandard Youngtabeller, en typ av Schur-funktion. Genom att använda Gelfand-Tstelinmönster som ett antal halvrum kan man bilda Gelfand-Tsetlinpolytoper. I den här uppsatsen undersöks de här polytoperna upp till en dimension av 21 och deras Ehrhart-polynom beräknas.

Contents

1 Introduction

Representation theory and combinatorics are two important areas of mathematics. Kostka numbers and Littlewood-Richardson coefficients appear in both [Nar06]. They have a close connection to symmetric functions and Schur functions.

One such symmetric Schur function are Gelfand-Tsetlin patterns [Sta01]. These patterns form $\mathcal{H}$-polytopes, and a conjecture states that the Ehrhart polynomials of so called Gelfand-Tstelin polytopes have non-negative rational coefficients [KTT04]. As far as we are aware, this conjecture have neither been proven or disproven.

In this thesis, we investigate the Ehrhart polynomials of Gelfand-Tsetlin polytopes. Using computational power, over 1800 Gelfand-Tsetlin patterns were generated, from which polytopes were created and their Ehrhart polynomials computed. A limitation of the computations is the CPU-time needed to get the h^*-polynomials needed to get the Ehrhart-polynomials. Only Ehrhart polynomials with positive coefficients was found.

The strucutre of thesis is as follows: the first section, Section 2, gives a background to polytopes and Ehrhart theory. Section 3, describes symmetric functions with regards to semistandard Young tableaux. Section 4, describes the bijection between semistandard Young tableaux and Gelfand-Tstelin patters, as well as introduces Gelfand-Tstelin polytopes. In Section 5, the method used to generate the Gelfand-Tstelin patterns and the Ehrhart polynomials are described. In the last section, Section 6, the results are presented.

2 Polytopes and Ehrhart theory

2.1 Polytopes

2.1.1 $\mathcal{H}$-polytopes and $\mathcal{V}$-polytopes

The definitions, theorems and lemmas in this section are exclusively taken from [Bra07].

We start by defining convex polytopes. For this we need the definition of convexity and convex hulls.

Definition 2.1. A subset $X \subseteq \mathbb{R}^n$ is *convex* if $\theta\mathbf{x} + (1-\theta)\mathbf{y} \in X$ for every $\mathbf{x}, \mathbf{y} \in X$ and $\theta \in [0,1]$.

Definition 2.2. Given a finite set $Y \subseteq \mathbb{R}^n$, the *convex hull* of Y, denoted $\operatorname{conv}\{Y\}$, is the intersection of all convex sets containing Y, i.e.

$$\operatorname{conv}\{Y\} = \left\{ \sum_{\mathbf{y}\in Y} a_y \mathbf{y} : a_y \in \mathbb{R}_{\geq 0}, \sum_{y \in Y} a_y = 1 \right\}.$$

There are two ways to define polytopes; these are using halfspaces to define $\mathcal{H}$-polytopes or using vertices to define $\mathcal{V}$-polytopes. We show in Section 2.1.2 that these definitions are in fact equal.

We start by defining polytopes using halfspaces.

Definition 2.3. A *halfspace* in $\mathbb{R}^n$ is the set of solutions to a linear inequality of the form $\mathbf{a} \cdot \mathbf{x} \leq b$ where $\mathbf{a} \in \mathbb{R}^n$ and $b \in \mathbb{R}$.

Definition 2.4. An *affine subspace* $A \subseteq \mathbb{R}^n$ of dimension d is a translate by some fixed $\mathbf{y} \in \mathbb{R}^n$ of a d-dimensional linear subspace of $\mathbb{R}^n$.

Definition 2.5. Given a subset $V \subseteq \mathbb{R}^n$, the *affine span* of V, denoted $\operatorname{aff}(V)$, is the intersection of all affine subspaces of $\mathbb{R}^n$ containing V.

Halfspaces, affine subspaces and affine spans are linked by the following theorems.

Theorem 2.1. *The affine span of a subset of $\mathbb{R}^n$ is an affine subspace.*

Proof. Since affine subspaces are translates of linear subspaces, they satisfy the condition that if $\mathbf{x}, \mathbf{y} \in A$, $b \in \mathbb{R}$ for some affine subspace A, then $b\mathbf{x} + \mathbf{y} \in A$.

Now, assume there exists $\mathbf{x} \in \mathbf{y} \in V$. Then for any affine subset containing V there must exist $b\mathbf{x} + \mathbf{y}$. Thus, $b\mathbf{x} + \mathbf{y}$ is also in the intersection of all affine subsets containing V and the affine span of V is an affine subset. □

Theorem 2.2. *The boundary of any halfspace in $\mathbb{R}^n$ is an affine subspace of dimension $n - 1$.*

Proof. If the boundary contains the vectors $x, y \in \mathbb{R}^n$, it also contains $b\mathbf{x} + \mathbf{y}$ for some $b \in \mathbb{R}$. This is because any vector in the boundary can be scaled arbitrarily due to the boundary being infinite, and the addition of two vectors in the boundary can only create a vector also in the boundary. Thus, the boundary of a halfspace is an affine subspace.

Obviously, a halfspace in $\mathbb{R}^n$ have dimension n. The normal vector n for a halfspace points outwards from the halfspace, orthogonal to the boundary (see Figure 2.1). The boundary stretches infinitely out in all directions except the direction of the normal vector n. Thus, the boundary have a loss of one dimension compared to the halfspace.

We conclude the boundary of a halfspace is an affine set with dimension $n-1$. □

We use an example to demonstrate these properties.

Example 2.1. *The halfspace $H = \{x - y \leq 2 : (x, y) \in \mathbb{R}^2\}$ have the boundary $x - y = 2$, which is the 1-dimensional affine subspace $A = \{(x, x) + (0, -2) : x \in \mathbb{R}\} = \mathit{aff}(\{(0, -2), (2, 0)\})$, see Figure 2.1.*

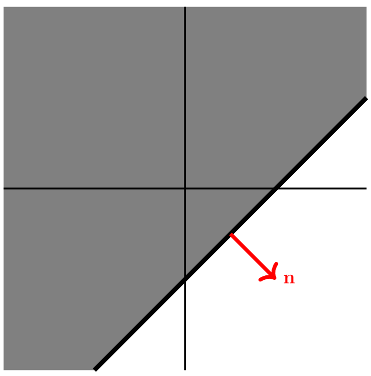

Figure 2.1: The halfspace $H = \{x - y \leq 2 : (x, y) \in \mathbb{R}^2\}$ in gray with its boundary marked using a thick line. Its normal vector n is the red arrow.

Finally, we have the definition for the first type of polytope.

Definition 2.6. An $\mathcal{H}$*-polytope* of dimension d in $\mathbb{R}^n$ is a bounded intersection P of a finite number of halfspaces in $\mathbb{R}^n$ such that P has affine span of dimension d.

Example 2.2. *The bounded intersection of the halfspaces* $H_1 = \{x+y \leq 1 : (x,y) \in \mathbb{R}^2\}$, $H_2 = \{x-y \leq 1 : (x,y) \in \mathbb{R}^2\}$ *and* $H_3 = \{3x-y \geq -1 : (x,y) \in \mathbb{R}^2\}$ *determine an* $\mathcal{H}$*-polytope. See Figure 2.2 for an illustration of this polytope.*

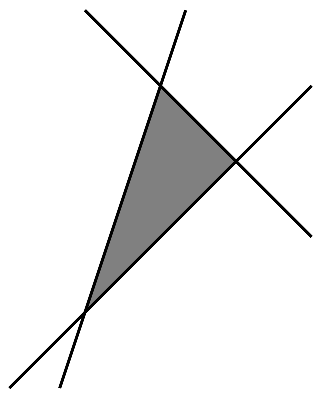

Figure 2.2: An $\mathcal{H}$-polytope.

Now we will give the second definition of polytopes.

Definition 2.7. A $\mathcal{V}$*-polytope* of dimension d in $\mathbb{R}^n$ is the convex hull P (denoted $\text{conv}\{V\}$) of a finite set of points $V \subset \mathbb{R}^n$ such that P has affine span of dimension d.

The subset of points in V on the boundary of the polytope is also called the *vertices* of the $\mathcal{V}$-polytope.

Example 2.3. *The convex hull of the set of points* $V = \{(0,1),(1,0),(-1,-2)\}$ *create a* $\mathcal{V}$*-polytope. See Figure 2.3 for a drawing of this polytope.*

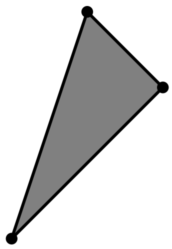

Figure 2.3: A $\mathcal{V}$-polytope.

As mentioned earlier, the set of $\mathcal{H}$-polytopes and the set of $\mathcal{V}$-polytopes are equal, as seen in the following theorem.

Theorem 2.3. *Any $\mathcal{V}$-polytope is also an $\mathcal{H}$-polytope. Similarly, any $\mathcal{H}$-polytope is also a $\mathcal{V}$-polytope.*

Proof. Read Section 2.1.2.

Example 2.4. *The polytopes in Example 2.2 and Example 2.3 are in fact the same polytope.*

The boundaries of polytopes are themselves polytopes itself of smaller dimensions. These are called *faces* and are defined as follows.

Definition 2.8. A linear inequality $a \cdot x \leq b$, where $a \in \mathbb{R}^n, b \in \mathbb{R}$, is *valid* for P if it is satisfied for all points $x \in P$. A *face* of P is any non-empty set of the form

$$F = P \cap \{x \in \mathbb{R}^n : a \cdot x = b\}$$

where $a \cdot x \leq b$ is a valid inequality for P. The *dimension* of a face is the dimension of its affine span.

Definition 2.9. Given a d-dimensional polytope P, the faces of dimension $d-1$ are called the *facets* of P. Given a d-dimensional polytope P, the faces of dimension 1 are called the *edges* of P. Given a d-dimensional polytope P, the faces of dimension 0 are called the *vertices* of P.

Example 2.5. *In Example 2.2, the hyperplanes are both the facets and the edges of the polytope, since the polytope is 2-dimensional and so the facets are 1-dimensional just like the edges. The vertices of the polytope are the 3 points where the hyperplanes intersect.*

We end this part by naming polytopes where the vertices are integers.

Definition 2.10. If $P = \text{conv}\{V\}$, where $V \subset \mathbb{Z}^n$, then P is called a *lattice polytope.*

2.1.2 Proof of equality between $\mathcal{V}$-polytopes and $\mathcal{H}$-polytopes

We stated in Theorem 2.3 that any $\mathcal{V}$-polytope is also an $\mathcal{H}$-polytope, and any $\mathcal{H}$-polytope is also a $\mathcal{V}$-polytope. In this section we prove this theorem. The definitions, theorems, lemmas and proofs in this section are taken from [Zie95].

We start with some definitions.

Definition 2.11. A *cone* is a non-empty set of vectors $C \subseteq \mathbb{R}^d$ that with any finite set of vectors, also contains all their linear combinations with nonnegative coefficients. In particular, every cone contains $\mathbf{0}$.

Definition 2.12. For an arbitrary subset $Y \subseteq \mathbb{R}^d$ we define its *conical hull* $\text{cone}(Y)$ as the intersection of all cones in $\mathbb{R}^d$ that contains Y.

We define that $\text{cone}(Y) = \{\mathbf{0}\}$ if Y is the empty set.

Definition 2.13. The *Minkowski sum* of two sets $P, Q \subseteq \mathbb{R}^d$ is defined to be

$$P + Q = \{\boldsymbol{x} + \boldsymbol{y} : \boldsymbol{x} \in P, \boldsymbol{y} \in Q\}.$$

Definition 2.14. An $\mathcal{H}$*-polyhedron* denotes an intersection of closed halfspaces, a set $P \subseteq \mathbb{R}^d$ presented in the form

$$P = P(A, \boldsymbol{z}) = \{\boldsymbol{x} \in \mathbb{R}^d : A\boldsymbol{x} \leq \boldsymbol{z}\}$$

for some $A \in \mathbb{R}^{m \times d}, \boldsymbol{z} \in \mathbb{R}^m$.

Definition 2.15. A $\mathcal{V}$*-polyhedron* denotes any finitely generated convex-conical combination: a set $P \subseteq \mathbb{R}^d$ that is given in the form

$$P = \text{conv}(V) + \text{cone}(Y)$$

for some $V \in \mathbb{R}^{d \times n}, Y \in \mathbb{R}^{d \times n'}$, as the Minkowski sum of a convex hull of a finite point set and the cone generated by a finite set of vectors.

Now we can define a $\mathcal{V}$-polytope simply as a *bounded* (contains no ray $\{\boldsymbol{u} + t\boldsymbol{v} : t \geq 0, \boldsymbol{v} \neq 0\}$) $\mathcal{V}$-polyhedron, and similary an $\mathcal{H}$-polytope is a bounded $\mathcal{H}$-polyhedron.

Thus, Theorem 2.3 follows if the theorem also is true for $\mathcal{H}$- and $\mathcal{V}$-polyhedrons. In order to prove that the theorem holds for polyhedrons, we first prove the case for cones.

Theorem 2.4. *A cone $C \subseteq \mathbb{R}^d$ is a finitely generated combination of vectors (a* $\mathcal{V}$-cone*)*

$$C = \textit{cone}(Y) \textit{ for some } Y \in \mathbb{R}^{d \times n}$$

*if and only if it is a finite intersection of closed linear halfspaces (an $\mathcal{H}$-*cone*)*

$$C = P(A, \mathbf{0}) \text{ for some } A \in \mathbb{R}^{m\times d}.$$

To prove Theorem 2.4, we need two lemmas, so we start by stating and proving the lemmas.

Lemma 2.1. *If $C = P(A, \mathbf{0})$ is an $\mathcal{H}$-cone in $\mathbb{R}^d$, then so is the* elimination *$elim_k(C) = \{\boldsymbol{x} - t\boldsymbol{e}_k : \boldsymbol{x} \in C, t \in \mathbb{R}\}$, and thus also the* projection *$proj_k(C) = elim_k(C) \cap H_k$ where $H_k = \{\boldsymbol{x} \in \mathbb{R}^d : x_k = 0\}$ is a hyperplane. Namely, we get $elim_k(C) = P(A^{/k}, \mathbf{0})$ for*

$$A^{/k} = \{\boldsymbol{a}_i : a_{ik}\} \cup \{a_{ik}\boldsymbol{a}_j + (-a_{jk})\boldsymbol{a}_i i : a_{ik} > 0, a_{jk} < 0\}.$$

(Here A and $A^{/k}$ are interpreted as sets of row vectors.)

Proof. We get that the row vectors in $A^{/k}$ are positive combinations of row vectors in A, and as such are the corresponding inequalities in C valid, so we get that $C \subseteq P(A^{/k}, \mathbf{0})$. Also, the variable x_k in the row vectors of $A^{/k}$ does not appear in the system $A^{/k}\boldsymbol{x} \leq \mathbf{0}$ since they are equal to zero by construction, which proves that $\text{elim}_k(C) \subseteq P(A^{/k}, \mathbf{0})$.

Now for the converse, we let $\boldsymbol{x} \in P(A^{/k}, \mathbf{0})$ and let $x_k = 0$. We claim that $\boldsymbol{x} - y\boldsymbol{e}_k \in C$ for suitable y. By using $\boldsymbol{x} - y\boldsymbol{e}_k$ in the system $A\boldsymbol{x} \leq \mathbf{0}$, we find that y has to satisfy

$$\max_i \left\{\frac{1}{a_{ik}}\boldsymbol{a}_i\boldsymbol{x} : a_{ik} > 0\right\} \leq y \leq \min_j \left\{\frac{1}{-a_{jk}}(-\boldsymbol{a}_j)\boldsymbol{x} : a_{jk} < 0\right\}.$$

This is satisfied if $a_{ik} > 0$ and $a_{jk} < 0$, since then $\frac{1}{a_{ik}}\boldsymbol{a}_i\boldsymbol{x} \leq \frac{1}{-a_{jk}}(-\boldsymbol{a}_j)\boldsymbol{x}$. This is equivalent to $(a_{ik}\boldsymbol{a}_j + (-a_{jk})\boldsymbol{a}_i)\boldsymbol{x} \leq 0$, which holds becase $\boldsymbol{x} \in P(A^{/k}, \mathbf{0})$. □

Lemma 2.2. *If $C = cone(Y)$ is a $\mathcal{V}$-cone in $\mathbb{R}^d$, then so is the intersection $C \cap H_k$. Namely, we get $C \cap H_k = cone(Y^{/k})$ for*

$$Y^{/k} = \{\boldsymbol{y}_i : y_{ki} = 0\} \cup \{y_{ki}\boldsymbol{y_j} + (-y_{kj})\boldsymbol{y}_i : y_{ki} > 0, y_{kj} < 0\}.$$

(Here Y and $Y^{/k}$ are interpreted as sets of columns vectors. Thus y_{ki} denotes the kth component of $\boldsymbol{y}_k$ and the (k, i)-entry of the matrix $Y = (\boldsymbol{y}_1, ..., \boldsymbol{y}_n)$).

Proof. All the vectors in $Y^{/k}$ have $x_k = 0$, so $C \cap H_k \supseteq \operatorname{cone}(Y^{/k})$.

For the reverse inclusion, consider some $\boldsymbol{v} = Y\boldsymbol{t} \in \operatorname{cone}(Y)$, where $\boldsymbol{t} \geq 0$ and $v_k = 0$. Now we have $t_i y_{ki} = 0$ for all i and we get $\boldsymbol{v} \in \operatorname{cone}(\{\boldsymbol{y}_i : y_{ki} = 0\})$, or we can expand $v_k = 0$ to get

$$K = \sum_{i:y_{ki}>0} t_i y_{ki} = \sum_{j:y_{kj}<0} t_j(-y_{kj}) > 0.$$

With this, we can rewrite $\boldsymbol{v}$ as

$$\begin{aligned}
\boldsymbol{v} &= \sum_{i:y_{ki}=0} t_i \boldsymbol{y}_i + \sum_{i:y_{ki}>0} t_i \boldsymbol{y}_i + \sum_{j:y_{kj}<0} t_j \boldsymbol{y}_j \\
&= \sum_{i:y_{ki}=0} t_i \boldsymbol{y}_i + \frac{1}{K} \sum_{i:y_{ki}>0} \left(\sum_{j:y_{kj}<0} t_j(-y_{kj}) \right) t_i \boldsymbol{y}_i \frac{1}{K} \sum_{j:y_{kj}<0} \left(\sum_{i:y_{ki}<0} t_i y_{ki}) \right) t_j \boldsymbol{y}_j \\
&= \sum_{i:y_{ki}=0} t_i \boldsymbol{y}_i + \sum_{\substack{i:y_{ki}>0 \\ j:y_{kj}<0}} \frac{t_i t_j}{K} \left((-y_{kj})\boldsymbol{y}_j + y_{ki}\boldsymbol{y}_j \right).
\end{aligned}$$

This gives an explicit representation of $\boldsymbol{v}$ as a conical sum of vectors in $Y^{/k}$, which proves the lemma. □

We are now prepared to prove Theorem 2.4.

Proof. For the direction from a $\mathcal{V}$-cone to an $\mathcal{H}$-cone, let $C = \operatorname{cone}(Y) \subseteq \mathbb{R}^d$ be a $\mathcal{V}$-cone. We can write it as

$$C = \{Y\boldsymbol{t} \in \mathbb{R}^d : \boldsymbol{t} \geq \boldsymbol{0}\} = \{\boldsymbol{x} \in \mathbb{R}^d : \exists \boldsymbol{t} \in \mathbb{R}^n : \boldsymbol{t} \geq \boldsymbol{0}, \boldsymbol{x} = Y\boldsymbol{t}\}.$$

Clearly, the set $\{(\boldsymbol{x}, \boldsymbol{t}) \in \mathbb{R}^{d+n} : \boldsymbol{t} \geq \boldsymbol{0}, \boldsymbol{x} = Y\boldsymbol{t}\}$ is an $\mathcal{H}$-cone. Thus $C = \operatorname{cone}(Y)$ can be written as the projection of this cone to the subspace $\{(\boldsymbol{x}, \boldsymbol{t}) \in \mathbb{R}^{d+n} : \boldsymbol{t} = 0\}$. This projection can be formed successively, by projecting with respect to individual t_k-coordinates one by one. This is proven in Lemma 2.1.

For the direction from an $\mathcal{H}$-cone to an $\mathcal{V}$-cone, let $C = P(A, \boldsymbol{0}) \subseteq \mathbb{R}^d$ be an $\mathcal{H}$-cone. We can write it as

$$\begin{aligned}
C &= \{\boldsymbol{x} \in \mathbb{R}^d : A\boldsymbol{x} \leq \boldsymbol{0}\} \\
&\cong \left\{ \binom{\boldsymbol{x}}{\boldsymbol{w}} \in \mathbb{R}^{d+m} : A\boldsymbol{x} \leq \boldsymbol{w} \right\} \cap \left\{ \binom{\boldsymbol{x}}{\boldsymbol{w}} \in \mathbb{R}^{d+m} : \boldsymbol{w} = \boldsymbol{0} \right\}.
\end{aligned}$$

Here, $\left\{ \binom{\boldsymbol{x}}{\boldsymbol{w}} \in \mathbb{R}^{d+m} : A\boldsymbol{x} \leq \boldsymbol{w} \right\}$ is a $\mathcal{V}$- cone, as shown above. The intersection with

$\left\{\binom{\boldsymbol{x}}{\boldsymbol{w}} \in \mathbb{R}^{d+m} : \boldsymbol{w} = \mathbf{0}\right\}$ can be formed successively, by setting coordinates to zero one at a time, i.e., intersecting with coordinate hyperplanes of the form $H_k = \{\boldsymbol{y} \in \mathbb{R}_{d+m} : y_k = 0\}$. This is proven in Lemma 2.2. □

We now present and prove the theorem for equality between $\mathcal{V}$-polyhedrons and $\mathcal{H}$-polyhedrons.

Theorem 2.5. *A subset $P \subseteq \mathbb{R}^d$ is a sum of a convex hull of a finite set of points plus a conical combination of vectors (a $\mathcal{V}$-polyhedron)*

$$P = conv(V) + cone(Y) \text{ for some } V \in \mathbb{R}^{d\times n}, Y \in \mathbb{R}^{d\times n}$$

if and only if P is an intersection of closed halfspaces (an $\mathcal{H}$- polyhedron)

$$P = P(A, \boldsymbol{z}) \text{ for some } A \in \mathbb{R}^{m\times d}, \boldsymbol{z} \in \mathbb{R}^m.$$

Proof. This theorem can be proven directly from Theorem 2.4. To do this, we pass from affine d-space to linear $(d+1)$-space by adjoining an extra coordinate (which is the zeroeth coordinate, note that every cone C in Theorem 2.4, by definition, contains the origin $\mathbf{0}$), mapping the points $\boldsymbol{x} \in \mathbb{R}^d$ to the vector $\binom{1}{\boldsymbol{x}} \in \mathbb{R}^{d+1}$. This reduces this theorem to the special case where P is a cone.

To see this, we associate with every polyhedron $P \subseteq \mathbb{R}^d$ a cone $C(P) \subseteq \mathbb{R}^{d+1}$ such that if $P = P(A, \boldsymbol{z})$ is an $\mathcal{H}$-polyhedron, we define

$$C(P) = P\left(\begin{pmatrix} -1 & \mathbb{O} \\ -\boldsymbol{z} & A \end{pmatrix}, \binom{0}{\mathbf{0}}\right).$$

That is, if P is defined by the inequalities $\boldsymbol{a}_i\boldsymbol{x} \leq z_i$, then $C(P)$ is defined by the inequalities $-z_i x_+ \boldsymbol{a}_i \boldsymbol{x} \leq 0$, together with the inequality $x_0 \geq 0$. We see that $C(P)$ is again an $\mathcal{H}$-polyhedron in $\mathbb{R}^{d+1}$ and

$$P = \left\{\boldsymbol{x} \in \mathbb{R}^d : \binom{1}{\boldsymbol{x}} \in C(P)\right\}.$$

Also, we see that if $P = P(B, \boldsymbol{u})$ is an arbitrary $\mathcal{H}$- polyhedron in $\mathbb{R}^{d+1}$, then $\{\boldsymbol{x} \in \mathbb{R}^d : \binom{1}{\boldsymbol{x}} \in P\}$ is an $\mathcal{H}$-polyhedron as well.

If $P = \text{conv}(V) + \text{cone}(Y)$ is a $\mathcal{V}$-polyhedron, we define

$$C(P) = \text{cone}\begin{pmatrix} \mathbb{1} & \mathbb{O} \\ V & Y \end{pmatrix}.$$

Then, $C(P)$ is again a $\mathcal{V}$-polyhedron in $\mathbb{R}^{d+1}$ and

$$P = \left\{ \boldsymbol{x} \in \mathbb{R}^d : \binom{1}{\boldsymbol{x}} \in C(P) \right\}.$$

Conversely, if $C = \text{cone}(W)$ is any cone in $\mathbb{R}^{d+1}$ generated by vectors $\boldsymbol{w}_i$ with $w_{i0} \geq 0$, then $\{\boldsymbol{x} \in \mathbb{R}^d : \binom{1}{\boldsymbol{x}} \in C\}$ is a $\mathcal{V}$-polyhedron.

Now, given any $\mathcal{H}$-polyhedron P, we apply Theorem 2.4 to $C(P)$ to conclude that $C(P)$ is a $\mathcal{V}$-cone contained in $\{\boldsymbol{x} \in \mathbb{R}^{d+1} : x_0 \geq 0\}$, so P is a $\mathcal{V}$-polytope as well. Conversely, if P is a $\mathcal{V}$-polyhedron, then accoring to Theorem 2.4 the associated cone $C(P)$ is a $\mathcal{H}$-polyhedron and so is P. □

We stated earlier that we can define a $\mathcal{V}$-polytope simply as a bounded $\mathcal{V}$-polyhedron, and similary an $\mathcal{H}$-polytope is a bounded $\mathcal{H}$-polyhedron. This means that we can apply Theorem 2.5 to polytopes, and Theorem 2.3 is thus proven.

2.2 Ehrhart theory

2.2.1 Rational generating functions

In order to introduce Ehrhart theory and Ehrhart polynomials, we first need a definition and lemma about rational generating functions of a single variable, see [Bra07].

Definition 2.16. The *generating function* for a sequence $\{a(k) : k \in \mathbb{Z}_{\geq 0}\}$ of complex values is the power series

$$\sum_{k \in \mathbb{Z}_{\geq 0}} a(k)x^k \in \mathbb{C}[[x]].$$

A *power series* is an infinite degree polynomial.

Lemma 2.3. *A function $f(t) : \mathbb{C} \to \mathbb{C}$ is a polynomial of degree d if and only if there exists complex values h_j^* such that*

$$\frac{\sum_{j=0}^{d} h_j^* x^j}{(1-x)^{d+1}} = \sum_{t \in \mathbb{Z}_{\geq 0}} f(t)x^t, \text{ and } \sum_j h_j^* \neq 0.$$

Proof. See Chapter 4 of [Sta11]. □

A consequence of Lemma 2.3 is that if we have a polynomial $f(t)$ of degree d

we can express it as

$$f(t) = \sum_{j=0}^{d} h_j^* \binom{t+d-j}{d},$$

where h_j^* are the coefficients in the numerator of the rational generating function for $f(t)$.

Example 2.6. *If we let $f(t) = 2t^2 + 2t + 1$, then*

$$\begin{aligned}
\sum_{t\in\mathbb{Z}_{\geq 0}} f(t)x^t &= 2\sum_{t\in\mathbb{Z}_{\geq 0}} t^2x^t + 2\sum_{t\in\mathbb{Z}_{\geq 0}} tx^t + \sum_{t\in\mathbb{Z}_{\geq 0}} x^t \\
&= 2\left(x\frac{d}{dx}\right)^2 \sum_{t\in\mathbb{Z}_{\geq 0}} x^t + 2\left(x\frac{d}{dx}\right)\sum_{t\in\mathbb{Z}_{\geq 0}} x^t + \sum_{t\in\mathbb{Z}_{\geq 0}} x^t \\
&= 2\left(x\frac{d}{dx}\right)^2 \frac{1}{1-x} + 2\left(x\frac{d}{dx}\right)\frac{1}{1-x} + \frac{1}{1-x} \\
&= \frac{2(x^2+x)}{(1-x)^3} + \frac{2(x-x^2)}{(1-x)^3} + \frac{(1-x)^2}{(1-x)^3} \\
&= \frac{1+2x+x^2}{(1-x)^3}.
\end{aligned}$$

Conversely,

$$\begin{aligned}
\frac{1+2x+x^2}{(1-x)^3} &= (1+2x+x^2)\sum_{t\in\mathbb{Z}_{\geq 0}} \binom{t+2}{2} x^t \\
&= \sum_{t\in\mathbb{Z}_{\geq 0}} \left(\binom{t+2}{2} + 2\binom{t+1}{2} + \binom{t}{2}\right) x^t \\
&= \sum_{t\in\mathbb{Z}_{\geq 0}} \left(\frac{(t+2)(t+1)}{2} + \frac{2(t+1)t}{2} + \frac{t(t-1)}{2}\right) x^t \\
&= \sum_{t\in\mathbb{Z}_{\geq 0}} (2t^2+2t+1)x^t.
\end{aligned}$$

2.2.2 Ehrhart polynomials

We introduce Ehrhart theory with lattice polytopes, using [Bra07] as source.

Definition 2.17. For P, a lattice polytope in $\mathbb{R}^n$ of dimension d and set

$$L_p(t) := |tP \cap \mathbb{Z}^n|$$

for $t \in \mathbb{Z}_{\geq 1}$. The *Ehrhart series of* P is

$$\mathrm{Ehr}_p(x) := 1 + \sum_{t \in \mathbb{Z}_{\geq 1}} L_p(t) x^t.$$

Theorem 2.6. *Let P, a lattice polytope in $\mathbb{R}^n$ of dimension d. There exist complex values $h_j^*, 0 \leq j \leq d$, such that the Ehrhart series for P is a rational generating function of the following form:*

$$Ehr_p(x) = \frac{\sum_{j=0}^{d} h_j^* x^j}{(1-x)^{d+1}}, \quad \sum_j h_j^* \neq 0.$$

Proof. Check sources of dissertation for all proofs.

Corollary 2.1. *$L_p(t)$ is expressible as a polynomial of degree d in the variable t.*

Proof.

Definition 2.18. The polynomial in Corollary 2.1 is called the *Ehrhart polynomial* of P and also denoted by ${}_p(t)$. The vector $(h_0^*, h_1^*, ..., h_d^*)$ of coefficients of the numerator of $\mathrm{Ehr}_p(x)$ is called the *h-star vector* for P.

Definition 2.19. Given a d-dimensional lattice polytope $P \subset \mathbb{R}^n$, rhe *relative volume* of a facet F of P is

$$\mathrm{relvol}(F) := \lim_{t\ to\infty} \frac{1}{t^{d-1}} |tF \cap \mathbb{Z}^n|.$$

Theorem 2.7. *For any d-dimensional lattice polytope P, the h^*-vector of P satisfies $(h_0^*, ..., h_d^*) \in (\mathbb{Z}_{\geq 0})^{d+1}$.*

These definitions and theorems concern lattice polytopes, but it was shown in [Ras04] that polytopes not necessarily need to be lattice for there to exist Ehrhart polynomials of the polytopes.

3 Symmetric functions

We start this section on symmetric functions by introducing, *semistandard Young tableaus*. The reason for this is that semistandard Young tableaus are in bijection with Gelfand-Tsetlin patters, as shown later in Section 4.1. We then continue through generalizing, introducing *Schur functions*, and some characteristics of Schur functions. The source for this part is [Sta01].

3.1 Semistandard Young tableaus

Definition 3.1. A *semistandard Young tableau* (SSYT) of *shape* λ is an array $T = (T_{ij})$ of positive integers such that it is weakly increasing in every row and strictly increasing down in every column.

Definition 3.2. The *size* of an SSYT is its number of entries.

We give an example to make SSYTs clearer.

Example 3.1. *Below is a SSYT of shape* $(5, 4, 2, 2)$*:*

$$\begin{matrix} 1 & 1 & 1 & 3 & 4 \\ 2 & 3 & 3 & 4 & \\ 3 & 4 & & & \\ 4 & 5. & & & \end{matrix}$$

As we can see it has 5 integers in the first row, 4 integers in the second row and 2 in the third and fourth row. It is also weakly increasing in the rows and strictly increasing in the columns.

Usually a SSYT is written as a Young diagram*, with boxes filled with positive integers as such*

1	1	1	3	4
2	3	3	4	
3	4			
4	5			

Definition 3.3. The SSYT T has the *type* $\alpha = (\alpha_1, \alpha_2, ...)$ if T has $\alpha_i = \alpha_i(T)$ parts equal to i.

Example 3.2. *The SSYT from earlier,*

1	1	1	3	4
2	3	3	4	
3	4			
4	5			

has type $(3, 1, 4, 4, 1)$ *since there are* 3 1*'s,* 1 2*'s etc.*

Definition 3.4. Let $\mu \subseteq \lambda$ such that $\mu_i \leq \lambda_i$ for all i. We define a semistandard Young tableau of *skew* shape λ/μ to be an array $T = (T_{ij})$ of positive integers of shape λ/μ that is weakly increasing in every row and strictly increasing in every column. What we mean by this definition is that the elements in the set μ are removed from the semistandard Young tableau, while all other rules apply as usual. We let an example demonstrate.

Example 3.3. *Below is a SSYT of shape* $(5, 4, 2, 2)/(2, 1)$*:*

		1	3	4
	3	3	4	
3	4			
4	5			

As we can see the SSYT is still weakly increasing in the rows and strictly increasing in the column. However, the first row is missing two integers in the beginning, and the second row is missing one integer in the beginning, since $\mu = (2, 1)$*.*

3.2 Schur functions

Semistandard Young tableaus are a combinatorial object underlying Schur functions.

Definition 3.5. We denote a *Schur function* as s_λ.

We continue by introducing some definitions, theorems and propositions for Schur functions, using SSYTs as examples.

Definition 3.6. Let λ/μ be a skew shape. The *skew Schur function* $s_{\lambda/\mu} = s_{\lambda/\mu}(x)$ of *shape* λ/μ in the variables $x = (x_1, x_2, ...)$ is the formal power series

$$s_{\lambda/\mu}(x) = \sum_T x^T,$$

summer over all SSYTs T of shape λ/μ. If $\mu = \emptyset$, we call $s_\lambda(x)$ the *Schur function* of shape λ.

Theorem 3.1. *For any skew shape λ/μ, the skew Schur function $s_{\lambda/\mu}$ is a symmetric function.*

Proof. This was shown by Cauchy in [Cau15]. □

Example 3.4. *All SSYTs of shape $(2,1)$ with the largest part being at most 3 are*

$$\begin{array}{|c|c|}\hline 1 & 1 \\ \hline 2 \\ \cline{1-1}\end{array}\quad \begin{array}{|c|c|}\hline 1 & 2 \\ \hline 2 \\ \cline{1-1}\end{array}\quad \begin{array}{|c|c|}\hline 1 & 1 \\ \hline 3 \\ \cline{1-1}\end{array}\quad \begin{array}{|c|c|}\hline 1 & 3 \\ \hline 3 \\ \cline{1-1}\end{array}\quad \begin{array}{|c|c|}\hline 2 & 2 \\ \hline 3 \\ \cline{1-1}\end{array}\quad \begin{array}{|c|c|}\hline 2 & 3 \\ \hline 3 \\ \cline{1-1}\end{array}\quad \begin{array}{|c|c|}\hline 1 & 2 \\ \hline 3 \\ \cline{1-1}\end{array}\quad \begin{array}{|c|c|}\hline 1 & 3 \\ \hline 2 \\ \cline{1-1}\end{array}\ ,$$

which gives the Schur function

$$s_{21}(x_1, x_2, x_3) = x_1^2 x_2 + x_1 x_2^2 + x_1^2 x_3 + x_1 x_3^2 + x_2^2 x_3 + x_2 x_3^2 + 2x_1 x_2 x_3.$$

It is easy to see that s_{21} is a symmetric function.

Definition 3.7. Let λ be a partition of some integer n and α a weak composition of n (i.e. a sum of non-negative integers adding up to n). The *Kostka number* $K_{\lambda\alpha}$ then denotes the number of SSYTs of shape λ and type α.

Definition 3.8. In a similar way we define the *skew Kostka number* $K_{\lambda/\mu,\alpha}$ as the number of SSYTs of shape λ/μ and type α.

Proposition 3.1. Suppose that μ and λ are partitions with $|\mu| = |\lambda|$ (i.e. they are the same size) and $K_{\lambda\mu} \neq 0$. Then $\mu \leq \lambda$, refered to as *dominance order*. Moreover, $K_{\lambda\lambda} = 1$.

Proof. It is obvious that there only exists one SSYT of type the skew shape λ/λ.

Consider the SSYT with the shape $(3,2,1)/(3,2,1)$. This is a SSYT with no integers, and this can only be done in one way. □

Example 3.5. *Consider the SSYT with $\lambda = (3,2,2)$, $\mu = (1,1)$, and $\alpha = (2,2,1)$. Then the Kostka number $K_{\lambda/\mu,\alpha} = 2$, since there are two possible SSYTs. These are*

$$\begin{array}{cc|c|c|}\cline{2-3} & 1 & 1 \\ \cline{2-3} & 2 \\ \hline \multicolumn{1}{|c|}{2} & 3 \\ \cline{1-2}\end{array}\quad \textit{and}\quad \begin{array}{cc|c|c|}\cline{2-3} & 1 & 2 \\ \cline{2-3} & 2 \\ \hline \multicolumn{1}{|c|}{1} & 3 \\ \cline{1-2}\end{array}\ ,$$

since they need to be strictly increasing in the columns and then we only have the choice of switching place on a 1 *and a* 2*.*

3.3 Littlewood-Richardson coefficients

Littlewood-Richardson coefficients appear in combinatorics in the theory of symmetric functions [Ras04].

Definition 3.9. The *Littlewood-Richardson coefficients* $c_{\lambda\mu}$ are the constants in the multiplication rule for Schur functions defined as

$$s_\lambda \cdot s_\mu = \sum_v c^v_{\lambda\mu} s_v. \tag{3.1}$$

4 Gelfand-Tsetlin

4.1 Gelfand-Tseltin patterns

The definition of the Gelfand-Tsetlin pattern is from [DLM04].

Definition 4.1. A *Gelfand-Tsetlin Pattern* or *GT-Pattern* is a triangular array $(x_{ij})_{1\leq i\leq j\leq n} \in \mathbb{R}^{\binom{n+1}{2}}$ satisfying the following inequalities:

- $x_{ij} \geq 0$, for $1 \leq i \leq j \leq n$; and
- $x_{i,j+1} \geq x_{ij} \geq x_{i+1,j+1}$, for $1 \leq i \leq j \leq n-1$,

where all $x_{ij} \in \mathbb{N}$.

We usually illustrate this pattern as

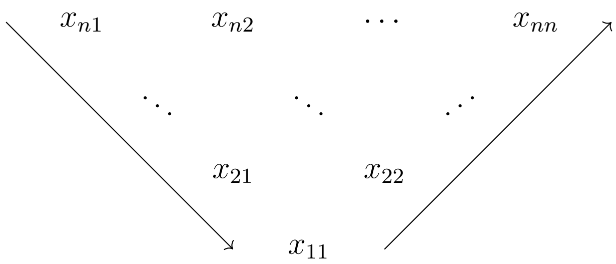

where the arrows indicate direction of less than or equal for the numbers.

Example 4.1. *This is an example of a GT-pattern:*

$$\begin{array}{ccccccccc} 6 & & 4 & & 3 & & 3 & & 1 \\ & 5 & & 4 & & 3 & & 1 & \\ & & 4 & & 4 & & 2 & & \\ & & & 4 & & 2 & & & \\ & & & & 2 & & & & \end{array}$$

Note how each value is less than or equal to the value above it on the left, and greater than or equal to the value above it on the right.

Now we reach the reason for introducing Schur functions in Section 3.

Theorem 4.1. *GT-Patterns are bijections with semistandard Young tableaus. The set of GT-patterns with top row $\lambda = [\lambda_1\ \lambda_2\ ...\ \lambda_n]$ is in bijection with the semistandard Young tableau of shape λ and maximal entry at most n.*

Proof. We start by showing that a semistandard Young tableau can be mapped to a Gelfand-Tsetlin pattern.

Given a semstandard Young tableau of shape $\lambda = [\lambda_1, \lambda_2, \ldots, \lambda_n]$ with type $\alpha = (\alpha_1, \alpha_2, \ldots, \alpha_k)$, a Gelfand-Tsetlin pattern can be formed with top row $\lambda = [\lambda_1, \lambda_2, \ldots, \lambda_n]$ and row sum differences $\alpha = (\alpha_1, \alpha_2, \ldots, \alpha_k)$.

That λ satisfies the conditions of a Gelfand-Tsetlin patters is because of the property of semistandard Young tableaus that forbids boxes in lower rows to have more columns than previous rows. This means that for a λ_i and λ_j in λ where $i > j$, $\lambda_i \geq \lambda_j$, which satisfies the condition for a top row of a Gelfand-Tsetlin pattern.

The type α for the semistandard Young tableau also satisfies the condition for row sum differences for a Gelfand-Tsetlin pattern. This is because $\sum_{i=1}^{n} \lambda_i = \sum_{j=1}^{k} \alpha_j$ by necessity, since all boxes in a semistandard Young tableau needs to be filled without any extra integers. This satisfies the condition of row sum differences for a Gelfand-Tsetlin pattern since the row sum differences needs to add up to the sum of λ. If they do not, the condition of inequalities in the Gelfand-Tsetlin pattern will not add up.

Thus, there is a mapping from any semistandard Young tableau to a Gelfand-Tsetlin pattern.

We now show that a Gelfand-Tsetlin pattern can be mapped to a semistandard Young tableau.

Given a Gelfand-Tsetlin pattern with top row $\lambda = [\lambda_1, \lambda_2, \ldots, \lambda_n]$ and row sum differences $\alpha = (\alpha_1, \alpha_2, \ldots, \alpha_k)$ there exist a semistandard young Tableau of shape $\lambda = [\lambda_1, \lambda_2, \ldots, \lambda_n]$ with type $\alpha = (\alpha_1, \alpha_2, \ldots, \alpha_k)$.

The top row λ of a Gelfand-Tsetlin pattern satisfies the condition of a semistandard Young tableau, because for any λ_i and λ_j where $i > j$, we have that $\lambda_i \geq \lambda_j$. This is exactly the condition for the rows of integers in a semistandard Young tableau, where the number of columns in each row needs to be the same amount or fewer than previous rows.

In order to get a correct Gelfand-Tsetlin pattern, we need that $\sum_{i=1}^{n} \lambda_i = \sum_{j=1}^{k} \alpha_j$. This means that the row sum differences α exactly adds up to the number of positions in a semistandard Young tableau of a shape λ. Moreover, in order to satisfy the condition of inequalities for a Gelfand-Tsetlin pattern, no row sum difference can be higher than λ_1. This means that they will satisfy the condition of a semistandard Young tableau being strictly increasing downwards.

Thus, a mapping from any Gelfand-Tsetlin pattern to a semistandard Young tableau exists.

We can conclude there is a bijection between Gelfand-Tsetlin patterns and semistandard Young tableaus. □

Remark 4.2. The type of the semistandard Young tableau can be read off from the GT-pattern, by examining the difference between the summation of the rows in the GT-pattern.

Lemma 4.1. *The Kostka number $K_{\lambda\alpha}$ of a SSYT is the same Kostka number for the corresponding number of Gelfand-Tsetlin patterns satisfying the top row λ with the row sum differences α.*

Proof. It follows from Theorem 4.1. □

We exemplify:

Example 4.2. *The GT-Pattern to the left corresponds to the semistandard Young tableau to the right:*

6		4		3		3		1
	5		4		3		1	
		4		4		2		
			4		2			
				2				

1	1	2	2	4	5
2	2	3	3		
3	3	4			
4	5	5			
5					

Note of how the first row in the GT-Pattern (from the bottom) have the row-sum 2*, and thus we have in the semi-standard Young tableau* 2 1*'s. The difference between the row sum of the first row and the second row in the GT-Pattern is* 4*, and so we have* 4 2*'s in the tableau.*

The number of boxes on each row are decided by the top row. We have for the GT-pattern that $\lambda = [6\ 4\ 3\ 3\ 1]$ *and thus for the SSYT we also get the shape* $\lambda = [6\ 4\ 3\ 3\ 1]$.

That a GT-pattern corresponds to a SSYT means that GT-patterns are Schur functions as well, and so the attributes for the Schur functions are also valid for GT-patterns.

4.2 Gelfand-Tsetlin polytopes

The GT-Pattern described in the previous Section 4.1 with its inequalities can be described as a $\mathcal{H}$-polytope. We again use a definition from [DLM04] and define

Definition 4.3. Given $\lambda, \mu \in \mathbb{Z}^n$, the *Gelfand-Tsetlin polytope* $GT(\lambda, \mu) \subset \mathbb{R}^{\binom{n+1}{2}}$ is the convex polytope of GT-patterns $(x_{ij})_{1\leq i\leq j\leq n}$ satisfying the equalities

- $x_{in} = \lambda_i$, for $1 \leq i \leq n$;
- $x_{11} = \mu_1$; and $\sum_{i=1}^{j} x_{ij} - \sum_{i=1}^{j-1} x_{i,j-1} = \mu_j$, for $2 \leq j \leq n$.

This is a polytope in $\mathbb{R}^{n(n+1)/2}$. The top row is λ and μ_j describes the jth row sum. We show this using an example.

Example 4.3. *Using the top row from the GT-pattern in Example 4.1 we have*

$$\begin{matrix} 5 & & 3 & & 1 \\ & x_{21} & & x_{22} & \\ & & x_{11} & & \end{matrix}$$

which gives us $\lambda = [5\ 3\ 1]$ *and we let the row sums be fixed as* $\mu_1 = 2$ *and* $\mu_2 = 5$. *This gives us the inequalities*

$$\begin{aligned} 5 \leq x_{21} \leq x_{11} \\ 3 \leq x_{22} \leq 1 \\ x_{21} \leq x_{11} \leq x_{22} \\ x_{21} + x_{22} = 5 \\ x_{11} = 2 \end{aligned}$$

and these define hyperplanes giving us an $\mathcal{H}$*-polytope.*

The GT-polytopes formed by GT-patterns are not necessarily lattice polytopes. This was shown in [DM04].

Proposition 4.1. *For a positive integer k, let $\lambda = (k^k, k-1, 0^k)$ and $\mu = ((k-1)^{k+1}, 1^k)$. Then a vertex of $GT(\lambda, \mu) \subset X_{2k+1}$ contains entires with denominator k*

Proof. See [DM04] for a complete proof. □

However, Rassart showed in [Ras04] that we still get Ehrhart-polynomials from these polytopes.

Theorem 4.2. *Let λ, μ be fixed partitions. The function*

$$P(k) = K_{k\lambda, k\mu}$$

is then the Ehrart function of the GT-polytope indexed by λ and μ. This is a polynomial.

Proof. See [Ras04] for a complete proof. □

The symmetric properties of the GT-pattern means that the same differences in $\mu_i - \mu_j$ where $i \neq j$, i.e. the differences between the summation of the rows of the GT-pattern, give rise to the same Ehrhart polynomial if we let λ be fixed.

In [KTT04] King, Tollu, and Toumazet stated three conjectures about the polynomials given by Schur functions. Following is the second conjecture (3.2) stated in their article.

Conjecture 4.4. *For all partitions λ, μ such that $K_{\lambda\mu} > 0$ there exists a polynomial $P_{\lambda\mu}(N)$ in N with non-negative rational coefficients such that $P_{\lambda\mu}(0) = 1$ and $P_{\lambda\mu}(N) = K_{N\lambda, N\mu}$ for all positive integers N.*

The first part is, as earlier stated, proven in [Ras04]. There does exist polynomials. However, the second part of the conjuecture, that these polynomials have non-negative coefficients, have as far as we know, not been proven.

The purpose of this thesis is to test the second part of Conjecture 4.4. We test it by generating GT-polytopes, computing their Ehrhart-polynomials and checking if any of those have negative coefficients. See Section 5 for method.

5 Method

5.1 Formalisation

GT-polytopes are represented as a row of integers, with a colon separating the integers into two groups. The integers before the colon represents the top row, and the integers after the colon represents the difference in row sum between the rows.

In order to create a correct GT-pattern, if the number of differences between row sums exceeds the number of rows created by the top row, zeros are added to the top row.

Example 5.1. *Consider the GT-polytope* 3 2 1 : 2 1 1 1 1*. In this case, we have 5 differences of row sum and thus 5 rows are required. The top row then becomes* $\lambda = [3\ 2\ 1\ 0\ 0]$*.*

The GT-pattern becomes

$$
\begin{array}{cccccccccc}
 & 3 & & 2 & & 1 & & 0 & & 0 \\
2 & & & & & & & & & \\
 & & x_{41} & & x_{42} & & x_{43} & & x_{44} & \\
 & 1 & & & & & & & & \\
 & & & x_{31} & & x_{32} & & x_{33} & & \\
 & & 1 & & & & & & & \\
 & & & & x_{21} & & x_{22} & & & \\
 & & & 1 & & & & & & \\
 & & & & & x_{11}. & & & & \\
 & & & & 1 & & & & &
\end{array}
$$

In the picture the differences between the row sums are indicated to the left between the rows. For the bottom row, the only variable $x_{11} = 1$ *by necessity, since the difference between no row* $(= 0)$ *and the only variable in the bottom row is* 1*.*

Continuing upwards we see that the sum for the fourth row from the bottom must be $x_{41} + x_{42} + x_{43} + x_{44} = 4$*. The difference between this row and the top row is* 2 *and the sum of the top row is indeed* $3 + 2 + 1 + 0 + 0 = 6$*.*

Some patterns can be ignored. We motivate these:

1. Two patterns with a fixed top row λ where the summation of the different row sums give the same Ehrhart polynomial.

2. If the row sum on the left of the colon is not the same as the sum on the right side, we do not get a correct Schur function.

3. If the difference between two row sums are larger than the greatest integer of the top row in the GT-pattern, i.e. if a number on the right side of a colon is greater than any of the numbers on the left side, we do not get a correct Schur function.

Motivation:

1. In Part 4.2 it was mentioned that the symmetric properties of Schur functions means that for a fixed top row λ, every GT-polytope where the summation of the different row sums give the same Ehrhart polynomial. This means that only one permutation of the row sum differences need to be checked, as all other permutations will give the same Ehrart polynomial.

2. If they do not add up to the same sum, there are two cases: (a) either the sum on the right side is smaller than on the left or (b) the sum on the right side is larger than on the left. By looking at the bijection between GT-patterns and SSYT's it is easy to see why neither of these cases works out.

   (a) In this case, we would have more boxes in the SSYT than numbers to fill them with.

   (b) In this case, we would have more numbers than boxes to fill them with.

   Neither case allows for a correct SSYT.

3. Once again looking at SSYT's, this is because we would have a greater number of integers of the same size than boxes, and in the downwards direction for a correct SSYT the integers are stricly increasing. Thus, any combination of integers where one or more integers on the right side of the colon was larger than any of the ones on the left side were excluded.

Example 5.2. *The GT-polytopes* $3\ 2\ 1\ :\ 2\ 1\ 1\ 1\ 1$ *and* $3\ 2\ 1\ :\ 1\ 1\ 2\ 1\ 1$ *give the same Ehrhart polynomial as they both have the top row* $\lambda = [3\ 2\ 1\ 0\ 0]$ *and the row sum differences are just permutations of each other.*

This is motivated by the fact that Schur functions are symmetric.

The GT-polytopes were generated by choosing an integer and computing all unordered partitions of that integer. These partitions became the top row and was ordered in descending order. Each of these partitions was then paired with all partitions having the greatest number equal to or less than the greatest number of the top row partitions, and these second partitions became the row sum differences.

Note that polytopes where the row sum differences where only ones where the sum of the top row was nine or ten were not calculated. Those had the most computational power needed to be calculated, and it was not possible with my computer, see Section 6.4.

5.2 Realization

The GT-polytopes were generated using Python[1]. Following the rules above, patterns for an integer n where the sum of the top row λ and the sum of the row sum differences both add up to n were created.

Following this, matrices were generated of each polytope in a format accepted by Julia. The Julia code then calculated the h^*-polynomial for each of the GT-polytopes.

Python was again used to get the Ehrhart polynomial from the h^*-polynomial.

[1] All code and data can be found at the Github repository for the project.

6 Results

6.1 Code and data

All code and data can be found on the github page github.com/oskarhogman/kandidatprojekt-matte in the folder `Code/`.

The layout of the folder `Code/` is as follows:

```
Code
├── ehrhart_files
│   ├── degrees
│   │   └── degree0.txt - degree21.txt
│   ├── GTP1.txt - GTP10d21.txt
│   └── all_ehrharts.txt
├── julia_input
│   └── GTP1.jl - GTP10.jl
├── julia_output
│   └── GTP1.txt - GTP10d21.txt
├── polytopes
│   └── GTP1.txt - GTP10.txt
├── GTP_generator.py
├── calculate_ehrhart.py
├── calculate_hstar.jl
├── collect_all_ehrhart_polynomials.py
├── collect_ehrharts_by_degree.py
├── create_julia_input.py
└── matrix_generator.py
```

The python-file `GTP_generator.py` creates patterns such as in Example 5.1 and puts them as text-files in the folder `polytopes`. Each text-file contain all possible combinations of polytopes, except for the skipped ones as stated in Section 5. The name `GTPa`, where `a` is an integer, is a short hand for *Gelfand-Tsetlin Polytope* with top row sum a.

The file `create_julia_input.py` make use of `matrix_generator.py` to create the files in the folder `julia_input`. Julia will read the matrices to create the polytopes.

The Julia-file `calculate_hstar.jl` read the files in `julia_input`, creates the polytopes, compute their h^*-polynomial and writes the data to the files in `julia_output`. Due to the polytopes in `GTP10` taking so much time (see 6.4), they were divided by dimension and computed for only one dimension at a time. The file `GTP10d10.txt` contains all polytopes of dimension 10 or lower.

The file `calculate_ehrhart.py` then takes the data in `julia_output` and from the h^*-polynomial computes the Ehrhart polynomial, which is stored in `ehrhart_files`. The file `collect_all_ehrhart_polynomials.py` then collected the polynomials such that each polynomial is related to all polytopes that gave that specific Ehrhart polynomial and saved in `all_ehrharts.txt`. This is because many polytopes gave the same Ehrhart polynomial.

The file `collect_ehrharts_by_degree` saves the Ehrhart polynomials by the dimension of polytope that created them instead, in the folder `ehrhart_files/degrees/`.

6.2 General results

In total 1830 Gelfand-Tsetlin polytopes were generated. The largest integer to partition was 10. These created 321 unique Ehrhart polynomials. None of them had a negative coefficient.

6.3 Polynomials

The lowest degree of an Ehrhart polynomial was 0. The highest was 21. As we can see in Table 1, the most common degree was 0 and the least common degree was 21 for the polynomials.

6.4 CPU-time

For the CPU-time for all files, see Table 2. Notice that even though the polytopes with top row sum 9 and 10 discard all polytopes where the row sum differences all are only 1, `GTP9` still matches `GTP8` in CPU-time and `GTP10` took 412.8 hours, or over 17 days to compute. The time for GTP10 is slightly skewed to the higher side, due to having to read in and compute the dimension of each polytope 12 times (once for each file), but by checking the files `GTP10da.txt` (where `a` is an integer) in the folder `julia_output.txt` we see that usually it took less than 0.1 seconds for each polytope to do that, so the computational cost is still for computing the h^*-polynomial.

Checking the files in `julia_output` we see that the polytope taking longest time to compute was 3 3 2 1 1 : 2 1 1 1 1 1 1 1 1 with a CPU-time of 458759.3045768738 seconds, or 127 hours. The shortest CPU-time for a computed polytope (where h^*-was able to be computed) was 5 1 1 1 1 1 : 4 3 3 with a CPU-time of 0.008860111236572266 seconds.

Table 1: Number of Gelfand-Tsetlin polytopes creating an Ehrhart polynomial of a certain degree

Ehrhart polynomial degree	**Number of GT-polytopes**
0	512
1	187
2	190
3	162
4	134
5	113
6	80
7	60
8	64
9	43
10	26
11	44
12	23
13	11
14	18
15	13
16	8
17	4
18	2
19	4
20	2
21	1

Table 2: Gelfand Tsetlin polytope file and the CPU-time to compute them

GT-polytope file	**CPU-time (seconds)**
GTP1	0.8613970279693604
GTP2	0.6129059791564941
GTP3	0.3842151165008545
GTP4	1.2566630840301514
GTP5	3.4246909618377686
GTP6	9.191021919250488
GTP7	23.879514932632446
GTP8	225.41200995445251
GTP9	219.7667908668518
GTP10	1486141.4541709423

References

[Bra07] Benjamin James Braun. *Ehrhart theory for lattice polytopes.* PhD thesis, Washington University, 2007.

[Cau15] Augustin Louis Cauchy. Mémoire sur les fonctions qui ne peuvent obtenir que deux valeurs gales et de signes contraires par suite des transpositions opres entre les variables qu'elles renferment. *J. Ec. Polytech*, 1:4, 1815.

[DLM04] Jesús A De Loera and Tyrrell B McAllister. Vertices of gelfand–tsetlin polytopes. *Discrete & Computational Geometry*, 32:459–470, 2004.

[DM04] Jesús A. De Loera and Tyrrell B. McAllister. Vertices of Gelfand–Tsetlin polytopes. *Discrete & Computational Geometry*, 32(4):459–470, September 2004. doi:10.1007/s00454-004-1133-3.

[KTT04] R. C. King, C. Tollu, and F. Toumazet. Stretched Littlewood–Richardson coefficients and Kostka coefficients. In P. Winternitz, J. Harnard, C. S. Lam, and J. Patera, editors, *Symmetry in Physics: In Memory of Robert T. Sharp*, volume 34, pages 99–112. AMS / OUP, 2004. URL: http://eprints.soton.ac.uk/41202/.

[Nar06] Hariharan Narayanan. On the complexity of computing kostka numbers and littlewood-richardson coefficients. *Journal of Algebraic Combinatorics*, 24(3):347–354, 2006.

[Ras04] Etienne Rassart. A polynomiality property for Littlewood–Richardson coefficients. *J. Comb. Theory Ser. A*, 107(2):161–179, August 2004. doi:10.1016/j.jcta.2004.04.003.

[Sta01] Richard P. Stanley. *Enumerative Combinatorics: Volume 2.* Cambridge University Press, first edition, 2001. doi:10.1017/CBO9780511609589.

[Sta11] Richard P. Stanley. *Enumerative Combinatorics: Volume 1.* Cambridge University Press, second edition, 2011. doi:10.1017/CBO9781139058520.

[Zie95] Günter M. Ziegler. *Lectures on polytopes.* Springer-Verlag, New York, 1995. URL: http://www.worldcat.org/search?qt=worldcat_org_all&q=9780387943657.